JOURNAL OF AEROSPACE SOCIETY MALAYSIA

ARTICLE

EXPERIMENTAL ASSESSMENT OF PROPELLER-DOWNWASH EFFECTS ON THE WING'S AERODYNAMIC CHARACTERISTICS AT LOW REYNOLDS NUMBER

Muhammad Aqil Karimi Mohd Sabri [1], Mohamad Izzat Truna [2], Mohd Rashdan Saad [2], Norzaima Nordin [2], Muhammad Amirul Adli Nor Zaidi [1] and Baizura Bohari [2,*]

1. Kulliyyah of Engineering, International Islamic University Malaysia, Kuala Lumpur, Malaysia.
2. Department of Aeronautic Engineering and Aviation, Faculty of Engineering, Universiti Pertahanan Nasional Malaysia, Kuala Lumpur, Malaysia.

*Correspondence: baizura@upnm.edu.my

Abstract: Unmanned aerial vehicles (UAVs) and micro air vehicles (MAVs), which are often referred to as drones, are among the advancing technologies that are utilized to secure remote surveillance. The propeller technology used by these aircraft has a considerable impact on their wing's aerodynamics. It has been shown that the propeller slipstream affects the pressure distribution over the wing surfaces in both chordwise and spanwise directions, influencing the distribution of wing loading especially during low-speed cruising. This study is done to examine the effects of propeller slipstream at low Reynolds numbers on several airfoils, namely NACA 0012, NACA 4415 and NACA 6712, concentrating on four key factors: type of airfoil, propeller diameter, propeller speed and distance between the propeller and the rectangular wing. Specifically, in the context of employing propellers for UAV applications, the goal is to evaluate if these parameters result in improvements and to analyze their impacts on lift, drag and lift-to-drag ratio. On the whole, the results imply that the propeller effect reduces lift and drag on most parameters discussed. However, the lift-to-drag ratio appears to increase on specific parameters. In this case, reducing the distance between the wing and the propeller leads to noticeable improvement in the lift-to-drag ratio. However, if the distance becomes extremely small, lift-to-drag ratio starts to decrease again.

Keywords: propeller slipstream; propeller diameter; propeller speed; propeller distance; NACA airfoils

1. Introduction

The application trend of Unmanned Aerial Vehicles (UAVs) in the industry has shown a significant increase, especially in recent years whereby they are mostly used for both civilian and military purposes [1]-[2]. UAVs often operate at low Reynolds number. In the aviation and aircraft operation, turboprop aircraft uses propellers as their source of thrust and it has been shown that employing propellers in air vehicles yields excellent performance at low speeds region [3]. The propeller functions by creating thrust through differences in pressure between the front and rear surfaces of its airfoil-shaped blades. It has been highlighted that the propeller diameter is a crucial factor in propeller design. Through a numerical analysis utilizing STAR CCM+, the effects from varying the propeller diameter on the thrust (speed) performance have been investigated. The findings indicate that larger diameters lead to decreased drag and this is attributed to the heightened thrust generated, resulting in reduced induced drag. It has been affirmed in several studies that enlarging the propeller diameter will enhance the wing's lift-to-drag ratio [5]-[7]. Furthermore, the research demonstrates that smaller diameters yield higher lift-to-drag ratio at

high angles of attack, whereas larger diameters exhibit superior lift-to-drag ratio at lower angles of attack for the same pitch.

Furthermore, the separation between the propeller and wing is also a critical factor that influences the generated lift and drag forces. Previous research study has indicated that the absence of a propeller significantly impacts aerodynamic properties, with the specific effects will vary based on the propeller's placement [8]. The study emphasizes the importance of the propeller-to-wing distance in preserving the aerodynamic qualities, highlighting that increasing this distance with multiple propellers can lead to a reduction in drag. Moreover, another study has explored how the vertical distance (Z position) between the propeller and the wing impacts the lift coefficient [9]. In this study, it has been found that increasing the vertical distance between the wing and the propeller results in a decrease in lift coefficient.

It should be noted that previous researches are predominantly focused on propeller effects at high Reynolds number levels in aircraft applications. Studies on the propeller diameter, distance and analysis typically center around single propeller and distributed propeller (DP) aircraft. Further research needs to be conducted on propeller applications in UAVs to enhance the understanding and also evidence for sustainable aviation practices.

2. Methodology

The objective of this research is to examine how the slipstream from a propeller impacts the wings of an aircraft with various types of airfoils under low Reynolds number conditions. This study analyzes the influence of the propeller on lift and drag coefficients across different airfoil designs, the impact of the distance between the propeller and the airfoil, the effects of varying propeller diameters on lift and drag, and the consequences of using different propeller RPMs on the aircraft performance. The tests have been carried out in the low-speed LW-9300R Subsonic Wind Tunnel, employing the three-force balance setup. This wind tunnel utilizes open-loop suction to generate simulated wind, reaching speeds up to 105 m/s. It is an open-loop suction-type wind tunnel with dimensions of 0.3 m (W) x 0.3 m (H) x 1.0 m (L). The considered range of Reynolds number (Re) in this study is between 5×10^4 to 9×10^4, which is defining the low Re regime. The propeller's RPM is adjusted between 1200 and 1800 to prevent stall, and accommodate the small-scale airfoil model within the wind tunnel. The distance between the propeller blade and the airfoil is varied from 4 cm to 7 cm.

Three airfoils used in this experiment are NACA 0012, NACA 4415 and also NACA 6712. The computer-aided design (CAD) model of these airfoils is developed using SOLIDWORKS software and then sliced using ULTIMAKER Cura. The detailed coordinates and data for these airfoils are provided in Table 1.

Table 1: Airfoil profile coordinates

Airfoil profile	Maximum thickness (%)	Maximum camber (%)	Maximum camber position (%)	Chord line (mm)	Wing span (mm)
NACA 0012	12.2	0	0.0	155	250
NACA 4415	15.0	4	40.2	155	250
NACA 6712	12.0	6	70.0	155	250

In the meantime, the propeller mounting setup comprises two distinct sections: the baseplate and the propeller mounting. The propeller mounting's center of radius is positioned 16 cm above the wind tunnel's ground level to align with the airfoil's center of gravity. The baseplate is also generously sized to match with the width of the wind tunnel's test section, ensuring stability during the testing. Both the propeller mounting and baseplate are manufactured using similar process as the airfoil models. Notably,

the baseplate is designed with 100% infill to enhance its weight and strength, ensuring it can withstand the wind speeds within the wind tunnel. Furthermore, an Arduino Nano microcontroller is applied to control the speed of the propeller in revolutions per minute (RPM). The RPM value is displayed on an LCD screen. The Arduino Nano reads input from the brushless DC motor (BLDC) GT2215 and uses PID (Proportional-Integral-Derivative) control to regulate the speed. A YUMO E6B2-CWZ3E Rotary Encoder is also incorporated for speed measurement and control. Table 2 provides the details on the components used in this setup while Figure 1 shows visual representation of the propeller setup.

Table 2: List of components and their function

Components	**Functions**
LCD Display unit	Display propellers' RPM
Control Switch	A potentiometer that controls the propellers' RPM
Arduino Nano	Microcontroller (programmed with PID controller).
YUMO E6B2-CWZ3E Rotary Encoder	Use to measure rotation position. Arduino Nano collects the rotation position data and converts it to rotation speed in RPM.
Brushless DC motor (BLDC)	A motor that is used to rotate the propeller. BLDC is connected to the encoder by a shaft for PID purposes.
Electronic Speed controller (ESC)	To control the speed of the brushless motor (no feedback). The ESC will receive PWM from Arduino Nano to spin the BLDC. ESC is also used to supply 5V to Arduino Nano.
LiPo Battery	Acts as a power source of the whole system. It supplies voltage to all the electronic components in the circuit ranging from 6.4V to 8.4V.

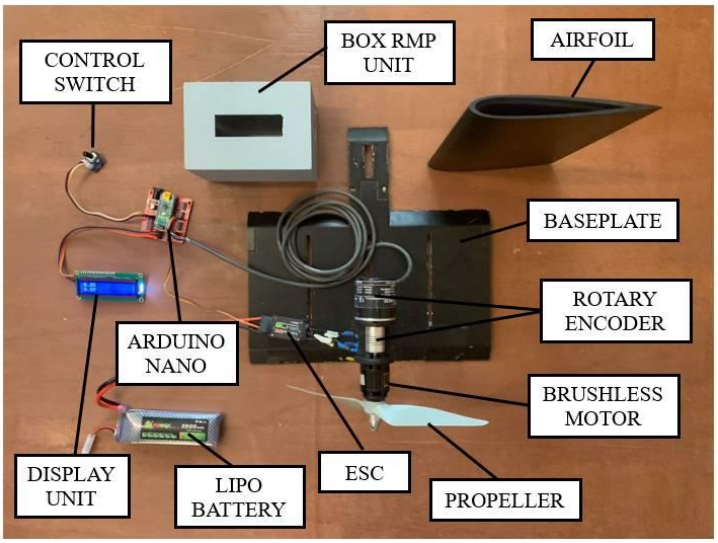

Figure 1: Propeller setup components

The configuration of the propeller arrangement in the wind tunnel is illustrated in Figure 2. The propeller's rotation speed can be adjusted externally using the control switch and it is monitored via the display unit.

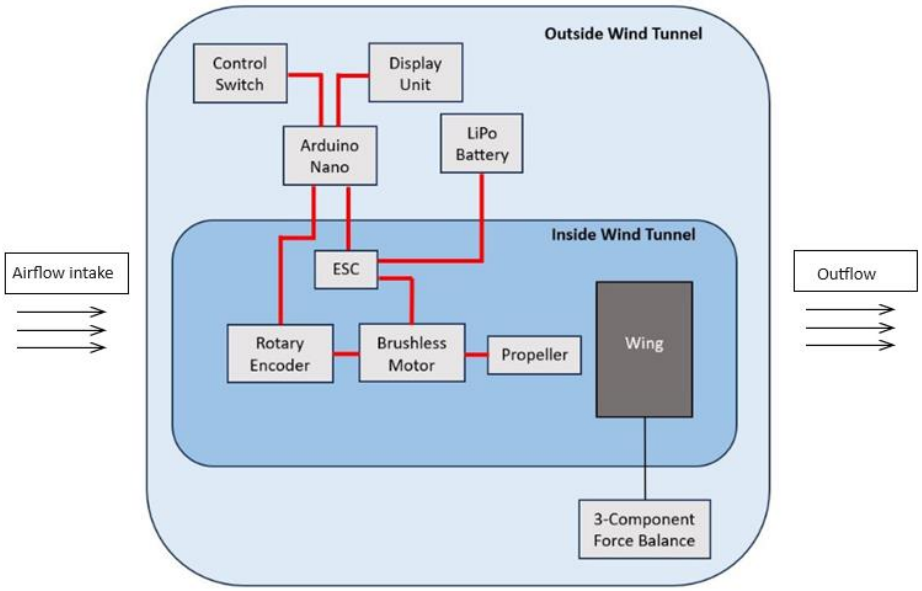

Figure 2: Diagram of the setup inside the wind tunnel

As mentioned before, this study aims to investigate four main factors: the impact of various airfoil types when subjected to the propeller effect, the influence of different propeller diameters, the effects of varying propeller speeds (measured in RPM) and the consequences of altering the distance between the propeller blade and the wing. The propeller configuration is positioned at a 5-cm distance from the airfoil, which is affixed to the force balance as depicted in Figure 3. The RPM meter and Arduino Nano circuit are located outside of the wind tunnel for monitoring and control purposes.

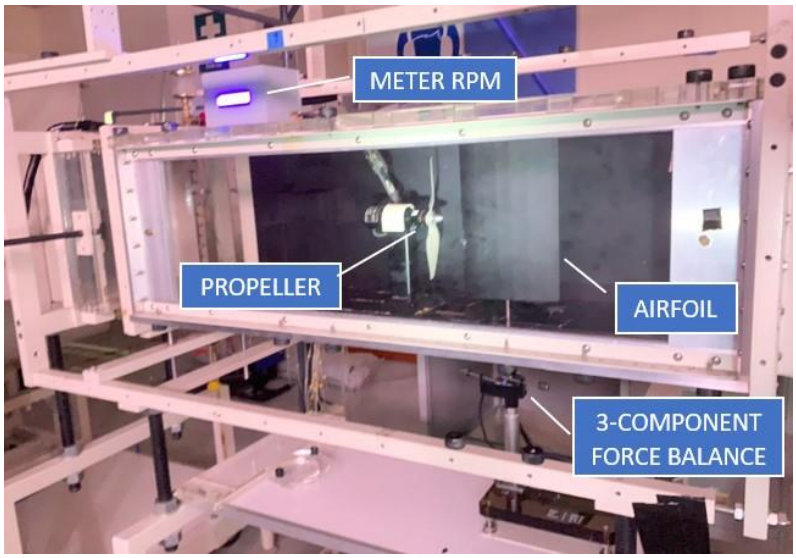

Figure 3: Experimental setup of propeller and airfoil

The variables considered in this experiment are the airfoil design, propeller size, propeller rotation speed (revolutions per minute or RPM), propeller position and Reynolds number. In each part of the experiment, Reynolds number is maintained as the primary constant parameter. Table 3 tabulates the constant parameters used throughout the experiment while Table 4 lists the dependent and independent variables for all the experiments performed.

Table 3: Constant parameters

Variable (units)	**Values**
Reynolds number	5.0×10^4, 6.0×10^4, 7.0×10^4, 8.0×10^4, 9.0×10^4
Angle of attack	0 degree
Wing chord line (mm)	155
Wing span (mm)	250

Table 4: Variables of the experiment

Independent Variables		**Dependent Variables**	
Airfoil Types	NACA 0012 NACA 4415 NACA 6712	**Wing Forces**	C_L C_D
Propeller Speed (RPM)	1200 RPM 1400 RPM 1600 RPM 1800 RPM		
Propeller Diameter (diameter x pitch)	7 x 6 inch 8 x 6 inch 9 x 6 inch	**Wing Performance**	C_L/C_D
Propeller Distance (cm)	4 cm 5 cm 6 cm 7 cm		

The first part of this study is to investigate the performance of the considered three airfoil types in terms of their suitability for flight operations, focusing on lift and drag coefficients. For this experiment, the propeller speed is set to 1200 RPM, propeller distance is set to 5 cm and propeller diameter is set to 7 x 6 inch. The airfoil models used in this experiment are shown in Figure 4. Based on the results of this first part of the study, the airfoil that exhibits the best performance as measured by its lift-to-drag ratio (C_L/C_D) is selected to be used in the subsequent part of the experiment.

NACA 6712 **NACA 4415** **NACA 0012**

Figure 4: Models for the three considered types of NACA airfoils

Next, only the selected best airfoil type is used in the second part of this study, which involves the experimental testing with varying propeller diameters while maintaining the propeller distance and RPM

as in the previous experimental setup (i.e. propeller speed is 1200 RPM and propeller distance is 5 cm). The goal of this second part of the investigation is to analyze the impact of different propeller diameters on the resultant lift and drag. Three propeller diameters are considered in this study as illustrated by the models depicted in Figure 5, namely 7 x 6 inch, 8 x 6 inch and 9 x 6 inch (i.e. the first number in the dimension denotes the propeller's diameter in inches while the second number refers to the pitch). The propeller model is affixed to the brushless DC motor (BLDC) shaft and consistent RPM is maintained throughout the duration of the experiment.

In the meantime, the third part of this experimental investigation is to study the impact of varying propeller speeds (RPM) on the selected best airfoil type. For this experiment, propeller distance is set to 5 cm and propeller diameter is set to 7 x 6 inch while the RPM is varied from 1200 up to 1800. The influence of RPM on the propeller's effectiveness in relation to the airfoil is assessed to understand its effect on lift and drag coefficients. RPM control is achieved through an Arduino Nano microcontroller programmed to regulate the BLDC input. RPM output is monitored and filtered using an encoder, with results displayed on the LCD screen. A potentiometer is utilized to adjust the RPM.

Lastly, the final part of this study is intended to examine the impact of varying the distance between the propeller blade and the wing, ranging from 4 cm to 7 cm, on lift and drag of the selected best airfoil type. This parameter is crucial in enhancing or diminishing the aerodynamic forces. To conduct this experiment, the propeller mounting is adjusted according to the specified distances. The experimental setup for the distance variation is illustrated in Figure 6. In this experiment, the propeller speed is set to 1200 RPM and propeller diameter is set to 7 x 6 inch.

Figure 5: Three different propeller diameters

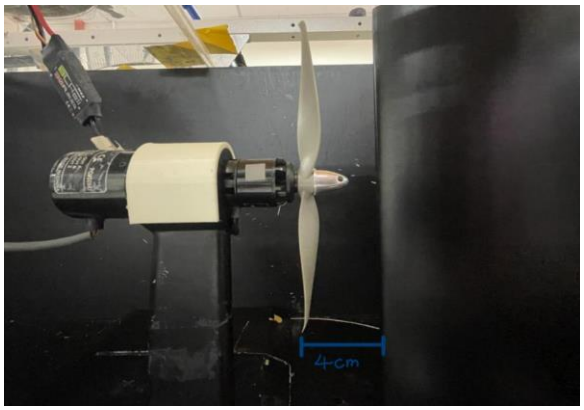

Figure 6: Setup for propeller distance effects

For all stages of this experimental study as described above, the same testing procedure is applied. The metal bar with a slotted wing is affixed using hot glue and clay, and then is connected to the three-force balance component to maintain the airfoil structure's stability during experiment. The propeller base is secured to the wind tunnel's floor upstream of the wing. All small electronic components and connections are positioned outside the wind tunnel and secured with tape to minimize any obstruction to the propeller or wing from the freestream flow. The distance between the propeller and wing can be adjusted by moving the propeller rig pole and adjusting the baseplate as needed. The propeller's desired radius is secured to the motor using an Allen key to prevent detachment during high-speed testing. The propeller is centered to ensure it is in a cruise condition. Once the propeller radius, distance between the propeller and wing, and also wing alignment have been established, the propeller speed is adjusted by manipulating the potentiometer until the desired value is displayed on the LCD screen. Subsequently, the freestream velocity within the wind tunnel is regulated by adjusting the wind tunnel's frequency. A brief pause of 5-10 seconds is implemented to ensure precise readings are captured. Following this, the

wind tunnel frequency is set to zero and the propeller speed is also brought to a halt. This sequence is then replicated for various speeds. The propeller is then removed and replaced with a different diameter propeller for subsequent experiments, following the same procedure. This process is also repeated for different distance configurations. Each experiment is conducted thrice to gather data for calculating the average results.

3. Results and Discussion

The first experimental stage is focused on examining the aerodynamic performance of the different considered airfoil types: NACA 0012, NACA 4415 and NACA 6712. As shown in Figure 7, the graph depicts the relationship between drag coefficient (C_D) and Reynolds number (Re) that is obtained from the experiment. The graph's findings highlight that NACA 0012 exhibited the lowest drag compared to the other airfoils. Additionally, it demonstrates an increasing trend in drag as Re is increased. Based on this, NACA 0012 airfoil can be recommended for flying at low Reynolds numbers due to its superior C_D performance. For NACA 6712 and NACA 4415 airfoils, their trends are quite similar. However, at lower Reynolds numbers, NACA 4415 airfoil has displayed lower drag when compared to NACA 6712. Both airfoils are therefore advised for flights within the Reynolds number range of 5 x 10^4 to 6 x 10^4 and the range of 8 x 10^4 to 9 x 10^4. For these two airfoils, operating outside of the regions would result in increased drag, which will diminish the aircraft's overall performance. All in all, when considering only the drag coefficient, NACA 0012 proves to be an optimal choice for minimizing drag, particularly when factoring in the propeller's effects.

Meanwhile, the lift coefficient vs Re plot, as depicted in Figure 8, also offers valuable insights. It reveals a consistent trend in lift coefficient across all airfoils. Notably, NACA 6712 and NACA 4415 airfoils have exhibited an increasing C_L as Re is increased. In contrast, NACA 0012 airfoil has displayed a decreasing C_L as Re increased. Among these three airfoils, NACA 6712 airfoil has stood out with an exceptional C_L performance compared to the other two airfoils. Consequently, NACA 6712 emerges as an excellent choice for achieving high lift when combined with the propeller's influence.

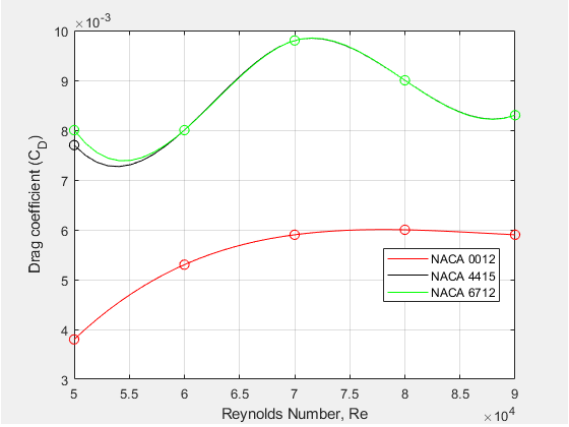

Figure 7: Drag coefficient, C_D against Re for different airfoil types

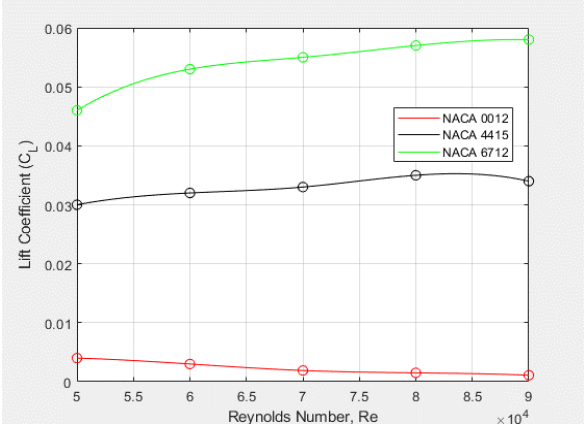

Figure 8: Lift coefficient, C_L against Re for different airfoil types

Furthermore, the C_L/C_D graph in Figure 9 shows that NACA 0012 airfoil exhibits a declining trend in terms of C_L/C_D as Reynolds number (Re) increases. This pattern suggests that the NACA 0012 airfoil might not be well-suited for flight operations. On contrary, both NACA 0012 and NACA 6712 airfoils show identical C_L/C_D ratios at Re = 5 x 10^4. However, it is advisable to avoid flight within the Re range of 6 x 10^4 to 8 x 10^4 as the C_L/C_D ratio decreases within this region for both airfoils. Beyond this range,

the flight performance for both airfoils generally remains satisfactory, except for the NACA 6712 airfoil that is not recommended for low Re (i.e. 5 x 10^4 to 5.5 x 10^4). Furthermore, it is important to note that NACA 6712 airfoil consistently achieves a higher maximum C_L/C_D ratio compared to NACA 4415 airfoil, indicating that NACA 6712 offers superior C_L/C_D performance for the flight operations when considering the propeller effect. In summary, NACA 6712 emerges as the most efficient NACA airfoil configuration for flight operations, primarily due to its consistently high C_L/C_D performance, and it is selected as the best airfoil type to be used for the experiments in the following stages of this study.

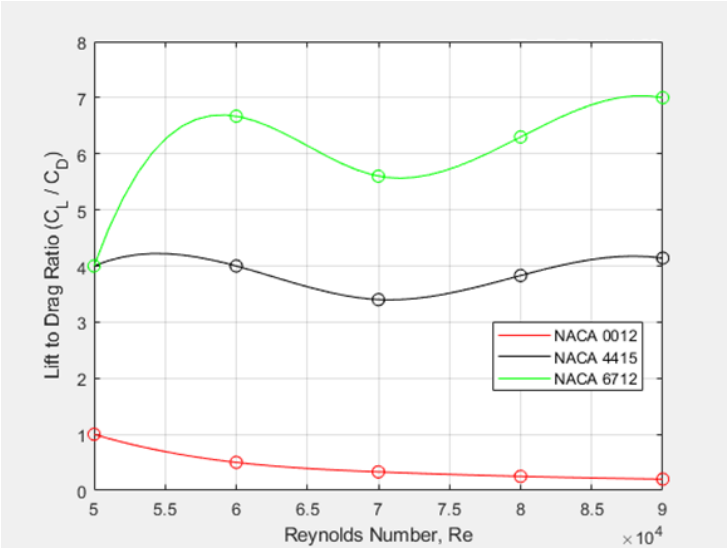

Figure 9: Lift-to-drag ratio, C_L/C_D against Re for different airfoil types

The second part of this experimental study us investigating the impact of propeller diameter on the wing's aerodynamic properties. The NACA 6712 airfoil, which is chosen based on the results from previous experiment, is used. The resultant C_D versus Re graph for the different propeller diameters is shown in Figure 10. It can be observed that C_D consistently decreases across all diameter configurations, within the Re ranges of 5 x 10^4 to 6 x 10^4 and 8 x 10^4 to 9 x 10^4, signifying excellent performance for flight operations within these regions. Hence each configuration should operate outside these specified regions as doing so will increase drag. Comparing the three propeller diameters, it is observed that for the lower Re range of 5 x 10^4 to 6 x 10^4, propeller diameter 7 x 6 inch has displayed considerably greater C_D than propeller diameter 9 x 6 inch. Conversely, within the Re range of 8 x 10^4 to 9 x 10^4, propeller 7 x 6 inch has demonstrated the lowest C_D while propeller 8 x 6 inch has exhibited the highest C_D. Apart from the mentioned regions, all diameter configurations displayed a consistent and similar trend with minimal differences in terms of C_D.

Figure 11 illustrates the C_L versus Re graph for the various propeller diameters. Across all diameter configurations, a consistent trend emerges, marked by an increasing C_L with respect to Re. This pattern indicates that C_L tends to be higher at higher Re values. However, it is important to note that operating within the lower Re range (i.e. 5 x 10^4 to 6 x 10^4) is discouraged due to significantly lower C_L values within this region. Apart from this specific region, all diameter configurations display a notable increase in C_L as Re increases, affirming the relationship between C_L and higher Re values. Notably, at Re of 8 x 10^4 to 9 x 10^4, the C_L for propeller diameter 8x6 surpasses that of other configurations. Meanwhile, propeller diameter 7 x 6 inch boasts the highest C_L at regions outside of 8 x 10^4 to 9 x 10^4. In terms of the C_L parameter, propeller diameter 7 x 6 inch appears to be a favorable choice for the flight operations, particularly at low Re values, as it consistently yields high C_L values across most Re regions below 9 x 10^4.

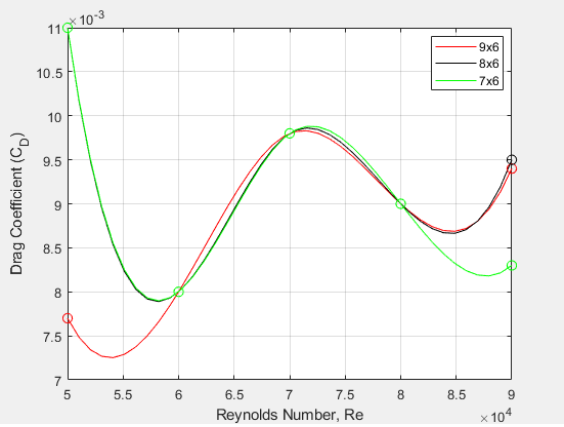

Figure 10: Drag coefficient, C_D against Re for different propeller diameters

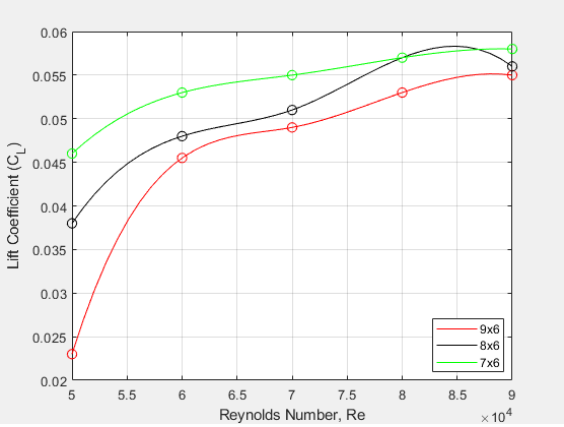

Figure 11: Lift coefficient, C_L against Re for different propeller diameters

Figure 12 displays the C_L/C_D data and related graph for various propeller sizes. Among the three propeller diameter configurations (7 x 6 inch, 8 x 6 inch, and 9 x 6 inch), specific regions stand out as favorable for flight operation. The regions include Re range between 5.5 x 10^4 to 6.5 x 10^4 and between 8 x 10^4 to 9 x 10^4, where C_L/C_D values exhibit a positive trend, signifying both increasing values and high performance. Thus, it is recommended to conduct the flight operations using any of these three propeller diameter configurations within these specified regions. Among the propeller diameters, 9 x 6 inch yields the highest C_L/C_D values in the recommended flight regions compared to others. On the other hand, the regions outside the mentioned ranges should be avoided for flight operations as they exhibit lower C_L/C_D values, which is indicative of diminished performance. Furthermore, it is observed that, as the propeller diameter increases, the propeller's effect becomes more pronounced, particularly at lower Re values for C_D. This aligns with previous research, which suggests that drag decreases with increasing diameter in low Re conditions (i.e. 5 x 10^4 to 6 x 10^4) [10]. As a result, the propeller's impact provides positive feedback for C_D at lower Re while being less effective at higher Re. The propeller with the lowest C_D at low Re (i.e. 5 x 10^4 to 6 x 10^4) shows that drag decreases with increasing diameter [4]. As the propeller diameter decreases, the wing's lift also rises [11]. It can be observed that increasing the propeller diameter will enhance the influence of propeller slipstream, which has a positive effect on C_D at low Re but a negative effect on C_L at most Re regions below 9 x 10^4. To conclude, propeller diameter of 7 x 6 inch is the most effective diameter for flight configuration since it has the highest C_L/C_D.

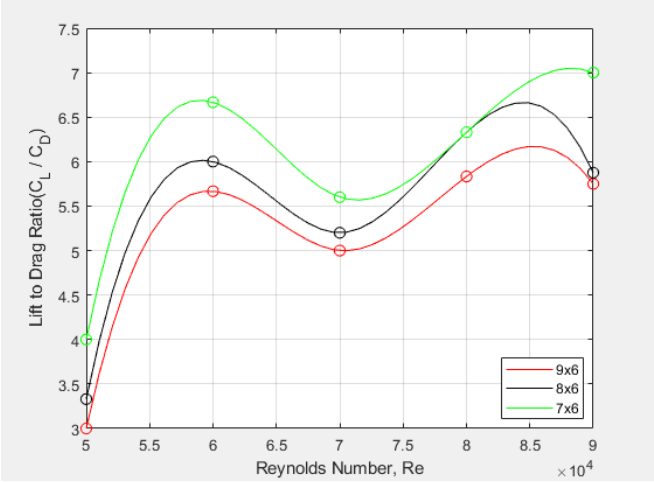

Figure 12: Lift-to-drag ratio, C_L/C_D against Re for different propeller diameters

Moreover, in the third stage of this experimental study, the effect under investigation is the impact of propeller speed on its aerodynamic characteristics. In this case, the speed is manipulated by using a potentiometer, which transmits the input to the Arduino Nano. Subsequently, a PID process is applied and the RPM value is displayed on the LCD screen. The propeller speed is varied as 1200 RPM, 1400 RPM, 1600 RPM and 1800 RPM. Figure 13 illustrates the graph of C_D versus Re for different RPM. At RPM of 1600, the drag coefficient exhibits a decrease within the Re range between 5 x 10^4 to 5.5 x 10^4 and between 8 x 10^4 to 9 x 10^4. Flying operations in these regions are recommended for the 1600 RPM setting since the drag coefficient is lower than in other regions. Conversely, for RPM settings of 1200 and 1800, flying within the Re range between 5.5 x 10^4 to 6.5 x 10^4 and between 8 x 10^4 to 9 x 10^4 is advisable. However, within the Re range between 8 x 10^4 to 9 x 10^4, the drag coefficient for 1200 RPM is significantly lower than 1800 RPM. To summarize, avoiding flying operations within the Re range of between 6 x 10^4 to 8 x 10^4 is advisable for all settings of the propeller speed. C_D increases significantly in this region compared to other regions below Re of 9 x 10^4.

Meanwhile, Figure 14 illustrates the relationship between lift coefficient and Re for various RPM settings. Each RPM setting exhibits a distinct C_L trend. Notably, as RPM increases, the trend becomes less stable and less distinct. Both 1400 RPM and 1600 RPM exhibit increasing trends but their C_L values in the lower Re range are considerably lower than those at 1200 RPM. As RPM increases further, C_L decreases across all Re values. At 1800 RPM, C_L decreases notably in the Re range between 5 x 10^4 to 6.5 x 10^4, indicating that the airfoil starts to stall at higher Re when the RPM is elevated. Additionally, C_L decreases in the Re range between 8 x 10^4 to 9 x 10^4. In summary, the configuration with low RPM settings consistently produces higher and more stable C_L values.

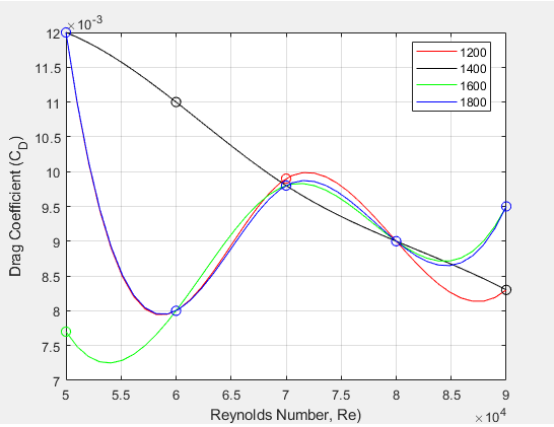

Figure 13: Drag coefficient, C_D against Re for different propeller speeds

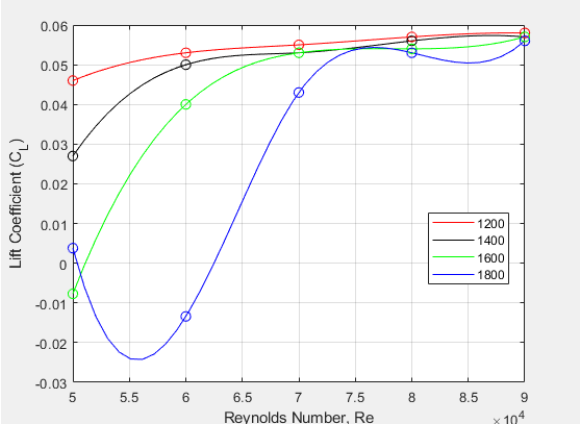

Figure 14: Lift coefficient, C_L against Re for different propeller speeds

As shown in Figure 15, all RPM settings exhibit consistent performance level of C_L/C_D values and trends within Re range between 7 x 10^4 to 8 x 10^4. In Re range between 5 x 10^4 to 7 x 10^4, the C_L/C_D trends for the RPM settings of 1200, 1400 and 1600 exhibit noticeable and consistent increase with the rising Re. Notably, among these settings, the 1200 RPM arrangement produces the greatest C_L/C_D. On the other hand, at RPM 1800, the C_L/C_D first decreases from Re of 5 x 10^4 to 5.5 x 10^4 before rising to Re of 7 x 10^4. This trend indicates that when the RPM value rises, flight operation performance gets unpredictable and the system becomes unstable. Within Re range between 8 x 10^4 to 9 x 10^4, the 1200 RPM and 1400 RPM settings demonstrate an increase in C_L/C_D as Re increases. On contrary, for the 1600 RPM setting, C_L/C_D increases until Re of 8.5 x 10^4 and then decreases until Re of 9 x 10^4. Notably, the 1800 RPM setting experiences a decline in C_L/C_D until Re of 8.5 x 10^4 and then witnesses an increase until Re of 9 x 10^4. In summary, these observations underscore that the higher RPM settings introduce

more significant fluctuations and reduced stability in flight operation performance, particularly within transition regions between different Reynolds numbers. A more comprehensive examination involving Particle Image Velocimetry (PIV) could be done to provide valuable insight into the flow characteristics of the same configuration across various RPM settings. Among the considered RPM configurations, RPM of 1200 emerges as the most optimal choice since it consistently yields the highest C_L/C_D across all Re ranges. This is aligned with the findings from another study that also shows an increase in RPM corresponds to increase in thrust coefficient, signifying that higher RPM levels intensify the propeller's influence on the airfoil [12].

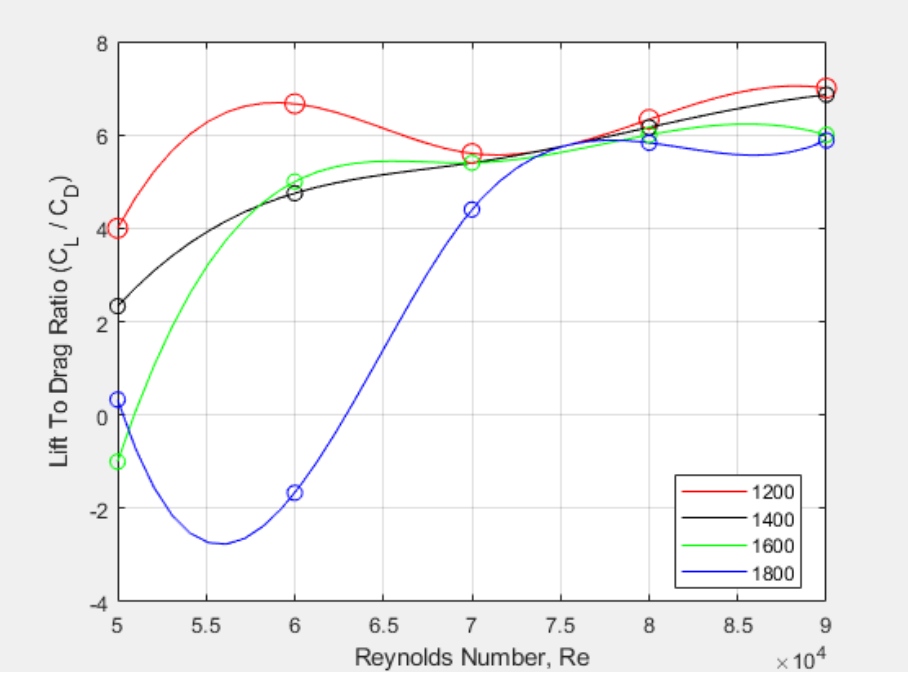

Figure 15: Lift-to-drag ratio, C_L/C_D against Re for different propeller speeds

Last but not least, the final experimental stage explores how the airfoil's aerodynamic characteristics are affected when the distance between the propeller blade and the airfoil is altered. This investigation examines distances ranging from 4 cm to 7 cm. It has been indicated that this distance parameter plays pivotal role in distributed propulsion systems, exerting large influence on aerodynamic performance compared to the number of propellers [8]. Therefore, investigating the impact of distance assumes significant importance in this context. Figure 16 illustrates the C_D versus Re graph for various distances. Interestingly, the 4 cm and 5 cm configurations exhibit no discernible difference in C_D. This outcome can be attributed to the limited scope of the small distance range explored in this experiment. For both 4 cm and 5 cm configurations, conducting flight operations within the Re regions between 6 x 10^4 to 8 x 10^4 and at Re of 9 x 10^4 is advisable. This is due to the low C_D values within this range, contributing to improved aircraft performance. Moving beyond this region for propeller distances of 4 cm and 5 cm is not recommended as it leads to increased drag, thereby diminishing the flight performance. It is also interesting to note that, at the 6 cm distance, C_D exhibits lower values at lower Re region (i.e. between 5 x 10^4 to 6 x 10^4) and Re = 9 x 10^4. Based on this analysis, it is evident that the closer the distance between the propeller and the airfoil, the lower the drag produced, especially at lower Re.

Additionally, Figure 17 shows the plot of C_L versus Re for various propeller distances. Across all configurations, the graph exhibits a consistent increasing trend in C_L with increasing Re. Notably, at the distance of 7 cm for all Re regions, the highest maximum C_L is attained compared to other settings. In the range of Re between 5 x 10^4 to 6 x 10^4, the 6 cm distance configuration boasts the highest C_L among

the considered options while 5 cm distance outperforms 4 cm distance in terms of C_L. With increasing Re up to 7 x 10^4, the 4 cm configuration experiences significantly higher C_L than 5 cm, whereas 7 cm maintains the highest C_L. As Re continues to rise to Re of 9 x 10^4, the lift of the 5 cm configuration once again increases, surpassing the C_L of the 4 cm configuration. However, for 6 cm and 7 cm, the C_L remains consistent. This analysis underscores that the furthest distance between the propeller results in the highest C_L. Conversely, as propeller distance decreases, C_L decreases and exhibits more fluctuations, rendering it less stable. Consequently, the configuration with the furthest distance proves to be optimal for generating high lift. It is advisable for aircraft to operate within the Re range of 7.5 x 10^4 to 9 x 10^4 since during this region, the lift generated is greater compared to the other regions, indicating excellent performance in flight operations.

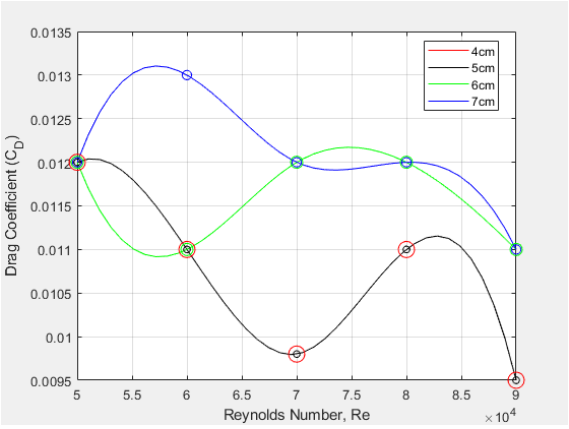

Figure 16: Drag coefficient, C_D against Re for different propeller distances

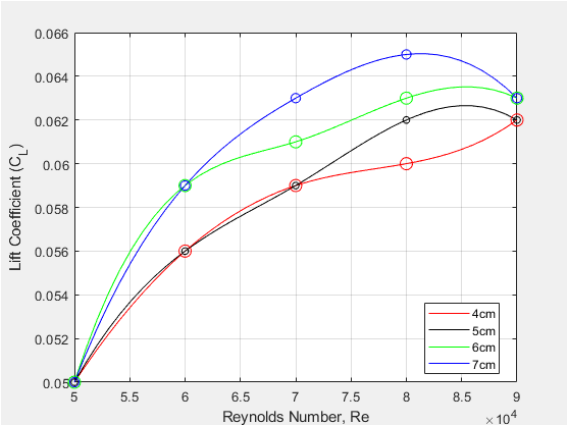

Figure 17: Lift coefficient, C_L against Re for different propeller distances

The plot of lift-to-drag ratio, C_L/C_D against Re, as depicted in Figure 18, reveals interesting insights. Initially, the configurations with 4 cm and 5 cm distances exhibit similar trends from Re range between 5 x 10^4 to 7 x 10^4. However, as Re continues to increase, the C_L/C_D for the 5 cm configuration surpasses that of the 4 cm configuration significantly. Consequently, it is advisable for both configurations to avoid flying within the Re range between 5 x 10^4 to 6.5 x 10^4 since the flight operation's performance in this region is suboptimal. In contrast, Re of 7 x 10^4 and 9 x 10^4 emerge as the optimal Re regions for both configurations in terms of flight operations. At these two points, higher C_L/C_D values are attained, indicating improved performance. In the meantime, the performance for 6 cm distance configuration exhibits significant variations across different Re regions. It experiences substantial increase in C_L/C_D at lower Re values (i.e. from 5 x 10^4 to 6 x 10^4), followed by a decrease until Re of 7.5 x 10^4, and then another increases up to Re of 9 x 10^4. On the other hand, the 7 cm configuration demonstrates favorable flight operation at Re range between 7 x 10^4 to 9 x 10^4, producing higher C_L/C_D values. On the contrary, the 7 cm configuration experiences a sharp decrease in C_L/C_D at lower Re values (i.e. from 5 x 10^4 to 6 x 10^4). On the whole, the analysis suggests that the 6 cm configuration performs exceptionally well at lower speeds (lower Re). In contrast, the 5 cm configuration is well-suited for higher Re operations below Re of 9 x 10^4. Reducing the distance between the propeller and the airfoil reduces drag [2]. This phenomenon occurs because the effect of the propeller slipstream is much stronger at closer distances. However, it is essential to note that reducing the distance also reduces C_L. Therefore, it becomes evident that the propeller slipstream's effect simultaneously reduces lift and drag. In distance configuration, the analysis indicates that the 5-cm distance setting offers the most optimal performance in C_L/C_D. This favorable outcome may be attributed to the more significant reduction in drag compared to the decrease in lift, suggesting that the propeller positively impacts the aerodynamic characteristics when considering different distance configurations.

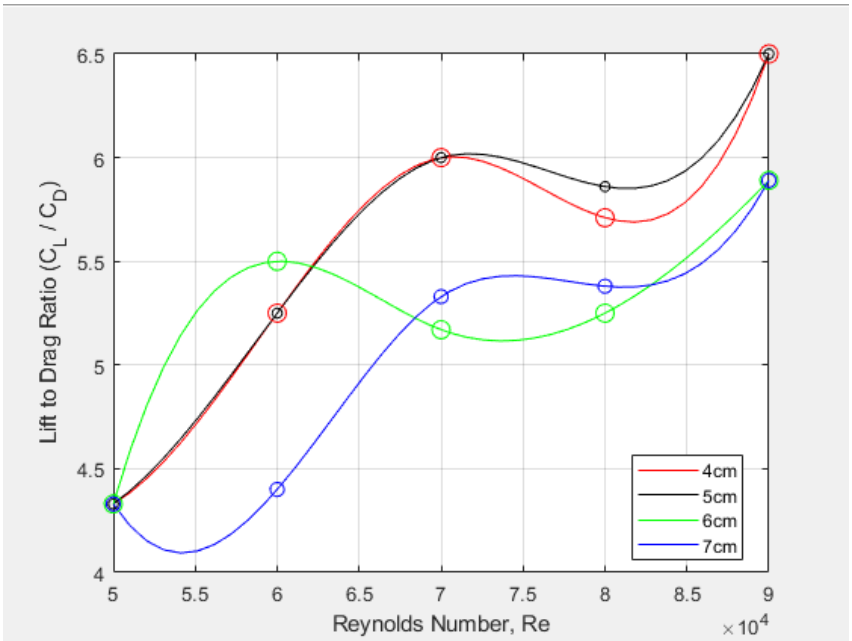

Figure 18: Lift-to-drag ratio, C_L/C_D against Re for different propeller distances

4. Conclusion

The impact of propeller slipstream on the aerodynamic performance varies depending on specific parameters. Positioning the propeller at a moderate distance, rather than too close, notably enhances the airfoil's lift-to-drag ratio. According to the results, the optimal configuration for propeller analysis at low Re involves small 7 x 6 inch diameter, low RPM setting of 1200 and 5 cm distance. Consequently, this configuration proves highly suitable for UAV applications due to its minimal space requirements for propeller diameter and low RPM, which eliminates the need for high-power supply. Moreover, the shorter distance reduces the overall size. While the propeller effect reduces both lift and drag, the drag reduction is more prominent and greatly improves the lift-to-drag ratio of the airfoil, especially when discussing the effect of distance.

Acknowledgement

The authors fully acknowledge the Ministry of Higher Education (MOHE), Malaysia and Universiti Pertahanan Nasional Malaysia for financial support to implement this research through the GPJP grant, UPNM/2020/GPJP/TK/11.

References

[1] R. W. Deters, G. K. A. Krishnan and M. S Selig, 'Reynolds Number Effects on the Performance of Small-Scale Propellers', Presented at 32nd AIAA Applied Aerodynamics Conference, Atlanta, USA, June 2014.

[2] K. Wang, Z. Zhou, X. Zhu and X. Xu, 'Aerodynamic Design of Multi-Propeller/Wing Integration at Low Reynolds Numbers', Aerospace Science and Technology, vol. 84, pp. 1-17, 2019.

[3] K. R. Moore and A. Ning, 'Distributed Electric Propulsion Effects on Existing Aircraft Through Multidisciplinary Optimization', Presented at AIAA/ASCE/AHS/ASC Structures, Structural Dynamics, and Materials Conference, Kissimmee, USA, January 2018.

[4] P. D. Vecchia, D. Malgieri, F. Nicolosi and A. De Marco, 'Numerical Analysis of Propeller Effects on Wing Aerodynamic: Tip Mounted and Distributed Propulsion', Transportation Research Procedia, vol. 29, pp. 106-115, 2018.

[5] C. Mingzhi, L. Kun, W. Chunqiang, W. Jingbo and Q. Zijie, 'Research on the Distributed Propeller Slipstream Effect of UAV Wing Based on the Actuator Disk Method', Drones, vol. 7, 2023.

[6] O. N. Vinogradov, A. V. Kornushenko, O. V. Pavlenko, A. V. Petrov, E. A. Pigusov and T. T. Ngoc, 'Influence of Propeller Diameter Mounted at Wingtip of High Aspect Ratio Wing on Aerodynamic Performance', Journal of Physics: Conference Series, vol. 1959, no. 1, 012051, 2021.

[7] F. Makino and H. Nagai, 'Propeller Slipstream Interference with Wing Aerodynamic Characteristics of Mars Airplane at Low Reynolds Number', Transactions of the Japan Society for Aeronautical and Space Sciences, vol. 12, 2014.

[8] D. Keller, 'Towards Higher Aerodynamic Efficiency of Propeller-Driven Aircraft with Distributed Propulsion', CEAS Aeronautical Journal, vol. 12, no. 4, pp. 777-791, 2021.

[9] G. J. Resende, V. Malatesta, M. C. Savio and B. M. Castro, 'Wing's Aerodynamic Characteristics due to Distributed Propulsion Over the Wingspan', Journal of the Brazilian Society of Mechanical Sciences and Engineering, vol. 45, no. 9, 2023.

[10] H. Zhu, Z. Jiang, H. Zhao, S. Pei, H. Li and Y. Lan, 'Aerodynamic Performance of Propellers for Multirotor Unmanned Aerial Vehicles: Measurement, Analysis and Experiment', Shock and Vibration, vol. 2021, pp. 1-11, 2021.

[11] E. A. Marcus, R. de Vries, A. R. Kulkarni and L. L. Veldhuis, 'Aerodynamic Investigation of an Over-the-Wing Propeller for Distributed Propulsion', Presented at AIAA Aerospace Sciences Meeting, Kissimmee, USA, January 2018.

[12] Z. Czyż, P. Karpiński, K. Skiba and M. Wendeker, 'Wind Tunnel Performance Tests of the Propellers with Different Pitch for the Electric Propulsion System', Sensors, vol. 22, no. 1, 2021.